

Short Communication

## Rich-grain-boundary PtRuNi with network structure as efficient catalysts for methanol oxidation reaction

Zi-ning Wang, Shu-hui Huo\*, Peng-xin Zhou\*

College of Chemistry and Chemical Engineering, Northwest Normal University, Lanzhou 730070, China

\*E-mail: [huosh\\_2000@163.com](mailto:huosh_2000@163.com), [zhoupx@nwnu.edu.cn](mailto:zhoupx@nwnu.edu.cn)

Received: 3 July 2019 / Accepted: 8 September 2019 / Published: 7 October 2019

Fabricating a network structure is an efficient way to increase the electrocatalytic activity of a catalyst. In this study, a network-like structure of PtRuNi with rich grain boundaries characterized *via* scanning electron microscopy and transmission electron microscopy was prepared by an electrochemical dealloying process. For methanol oxidation, PtRuNi networks show an onset potential of 0.40 V with a mass activity of 220 mA mg<sub>Pt</sub><sup>-1</sup> for methanol oxidation. The good catalytic activity of PtRuNi networks could be ascribed to the unique structure of a net framework with rich grain boundaries.

**Keywords:** PtRuNi; Nanoparticle; Catalyst; Direct methanol fuel cell.

### 1. INTRODUCTION

Direct methanol fuel cells (DMFCs) are efficient power devices in which chemical energy can be directly converted into electricity for portable and transportation applications. The electrochemical performance of DMFCs is mainly affected by catalysts [1]. Currently, carbon-supported Pt nanoparticles such as Pt/C from J.M. Corp. are believed to be the best commercial catalysts for DMFCs. However, this is not the most cost-effective catalyst for the large-scale application of DMFCs because of inherent shortcomings of scarcity, high price and toxicity [2, 3]. To meet potential market applications, there is a requirement to decrease noble metal loadings while improving the catalytic activity of the catalyst by fabricating an advanced structure and morphology, as well as by adding non-noble components.

Network-like nanostructures are promising structures for achieving a high utilization efficiency of precious metal electrocatalysts because they possess a porous framework due to their high active area, rich mass-transfer channels, and efficient electron mobility in metal ligands [4, 5]. A series of noble alloy networks, including PtNi, PtCo, and PdNi, were synthesized by various methods and

catalysed the reactions of either oxygen reduction or oxidation of small organic molecules [6-8]. Their high catalytic activities suggest that the network-like electrocatalysts are worthy of further development. Herein, a PtRuNi alloy is presented to increase the noble metal utilization of anode catalysts in DMFCs by both forming a network-like structure and adding the non-noble metal Ni. The PtRuNi network system is chosen for the following reasons: (i) PtRu is a well-known and most effective anode catalyst for methanol oxidation reaction (MOR), ensuring the PtRuNi with good MOR electrocatalytic performance [9]; (ii) Ni is an inexpensive transition metal and has a smaller atomic radius than Pt. Thus, strain is induced into the PtRuNi alloy, which makes it relatively active [10, 11]; and (iii) the network structure provides a large active area and favourable mass transfer, leading to enhanced catalyst efficiency.

## 2. EXPERIMENTAL

### 2.1 Preparation

All the chemicals used in this study were analytical grade, and were used directly from suppliers without any further purification. The commercial PtRu/C catalyst (20 wt.%) was purchased from J.M. Corp. First, 4 mg  $\text{NiCl}_2 \cdot 6\text{H}_2\text{O}$ , 44  $\mu\text{l}$   $\text{H}_2\text{PtCl}_6 \cdot 6\text{H}_2\text{O}$  solution (20 mg  $\text{mL}^{-1}$ ) and 11.4  $\mu\text{l}$   $\text{RuCl}_3 \cdot 6\text{H}_2\text{O}$  (20 mg  $\text{mL}^{-1}$ ) were added into ultrapure water (50 ml) with magnetic stirring. In this step, nitrogen is continuously introduced into the water. Afterward,  $\text{NaBH}_4$  solution (0.02 mol  $\text{l}^{-1}$ , 10 mL) was slowly introduced to the abovementioned solution and stirred for 30 min. Finally, the product was filtered out and rinsed with ultrapure water to neutrality and then stored in an ethanol solution.

### 2.2 Characterization

The morphology and structure of the products were investigated by transmission electron microscopy (TEM, JEM-2000FX, JEOL, Japan), scanning electron microscopy (SEM, Ultra Plus, Zeiss, Germany), and X-ray diffraction (XRD; D-3A, with  $\text{Cu-K}\alpha$  radiation,  $\lambda = 0.15418$  nm, Shimadzu, Japan).

### 2.3 Electrochemical measurements

Three-electrode system connected to electrochemical workstation (CHI 650D) was applied to investigate the electrocatalytic performance for these as-prepared products. In such three-electrode system, Pt wire was used as the counter electrode, Ag/AgCl (saturated KCl) as the reference electrode and glassy carbon (diameter 5 mm) as the counter electrode. The working electrode was fabricated as follows: 2 mg of the catalyst was dispersed in a 0.4 mL Nafion/ethanol (0.25% Nafion) solution. 8  $\mu\text{l}$  of the above solution was dropped onto the glassy carbon disc with a pipette. PtRuNi networks were achieved using cyclic voltammetry for 20 cycles in 0.1 M  $\text{HClO}_4$  over a potential range of 0.05-1.2 V (vs. RHE) with a scanning rate of 50  $\text{mV s}^{-1}$ .

### 3. RESULTS AND DISCUSSION

The XRD powder pattern of the PtRuNi networks is shown in Figure 1. Four characteristic diffraction peaks at  $2\theta \approx 40^\circ$ ,  $46^\circ$ ,  $68^\circ$  and  $82^\circ$  could be attributed to the (111), (200), (220) and (311) planes of the face-centred cubic structure respectively [12]. However, the PtRuNi precursor is amorphous, and the face-centred cubic structure was formed during the electrochemical dealloying process, which indicate the structural rearrangement to form orderly crystal structure was carried out with the dealloying. The morphology of the PtRuNi alloy characterized by SEM shown in Figure 1b is a uniformly network-like structure. The XRD and SEM results suggest that Ni metal flocculent was dissolved during the electrochemical dealloying, which also drive the structural rearrangement of PtRuNi simultaneously [13]. Figure 1c exhibited that the network structure consists of an aggregation of nanoparticles, which is further confirmed by TEM (Figure 1d). The nanoparticles in Figure 1e present irregular spherical shapes 10-15 nm in diameter, and they are linked to each other, resulting in the formation of rich grain boundaries. The high-resolution TEM image (Figure 1f) demonstrates that the surface of the PtRuNi nanoparticles has some breaches, resulting in an increase of the surface area.

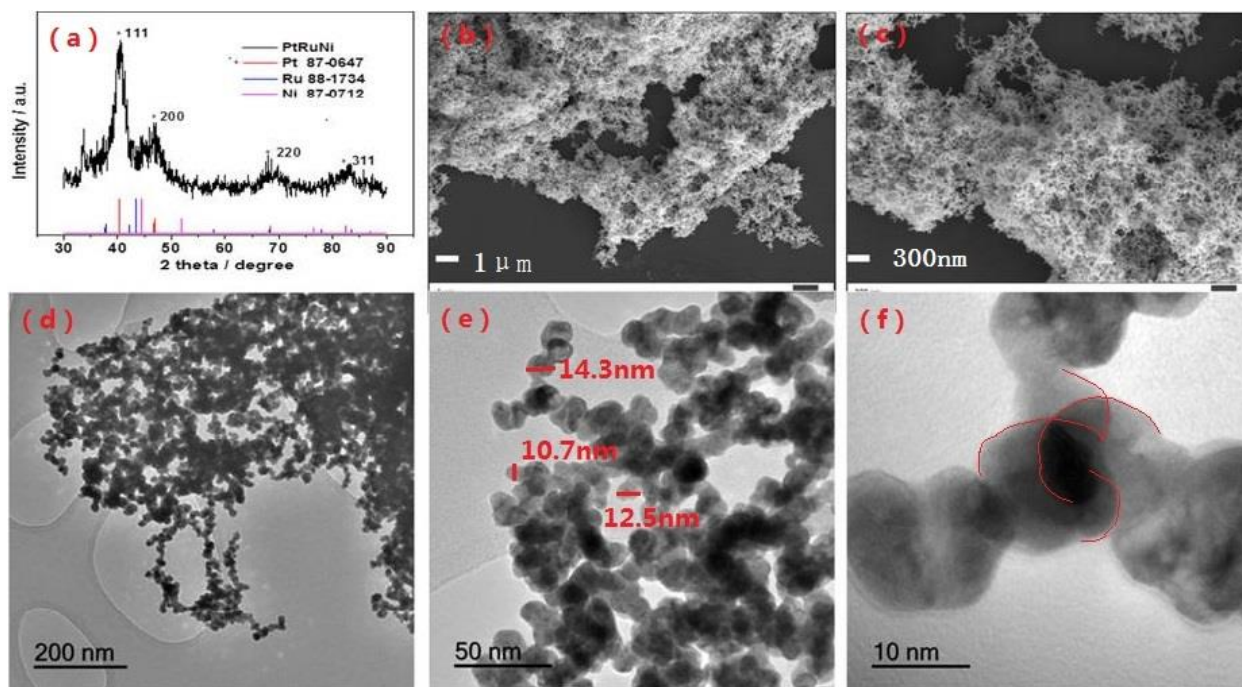


**Figure 1.** XRD pattern (a), SEM images (b and c), and TEM images (d-f) of PtRuNi networks.

The electrocatalytic performance of PtRuNi networks was first evaluated by cyclic voltammetry (CV). For comparison, data for commercial PtRu/C catalysts from J.M. Corp. are also presented here. CV was performed in nitrogen-purged 0.1 M HClO<sub>4</sub>, and the result is shown in Figure 2a. Three signals, namely, the hydrogen desorption/adsorption peaks, the electric double layer, and oxide formation/reduction peaks, appear for the two catalysts, which are consistent with the typical features of carbon-supported Pt-based electrocatalysts. The electrochemical surface area (ECSA) was

applied to indicate the utilization of Pt for Pt-based catalysts. The ECSA can be calculated based on following equations [14]:

$$ECSA \text{ (m}^2\text{g}^{-1}\text{Pt)} = Q_H / (2.1 \times m_{\text{Pt}}) \quad (1)$$

$$ECSA \text{ (m}^2\text{g}^{-1}\text{Pt)} = Q_{\text{CO}} / (4.2 \times m_{\text{Pt}}) \quad (2)$$

where  $Q_H$  (C) is the average charge of the hydrogen adsorption/desorption area,  $Q_{\text{CO}}$  (C) the average charge of the region of the CO oxidation peak area. The ECSAs are  $45.78 \text{ m}^2 \text{ g}_{\text{Pt}}^{-1}$  for PtRuNi networks and  $36.62 \text{ m}^2 \text{ g}_{\text{Pt}}^{-1}$  for PtRu/C catalysts. The ECSA of PtRuNi networks is 1.25 times larger than that of PtRu/C catalysts, suggesting that the PtRuNi networks have a higher catalytic efficiency than PtRu/C catalysts, leading to higher utilization of Pt. Table 1 shows that the ECSAs of the PtRuNi catalyst are at a moderate level compared with the reported catalysts.

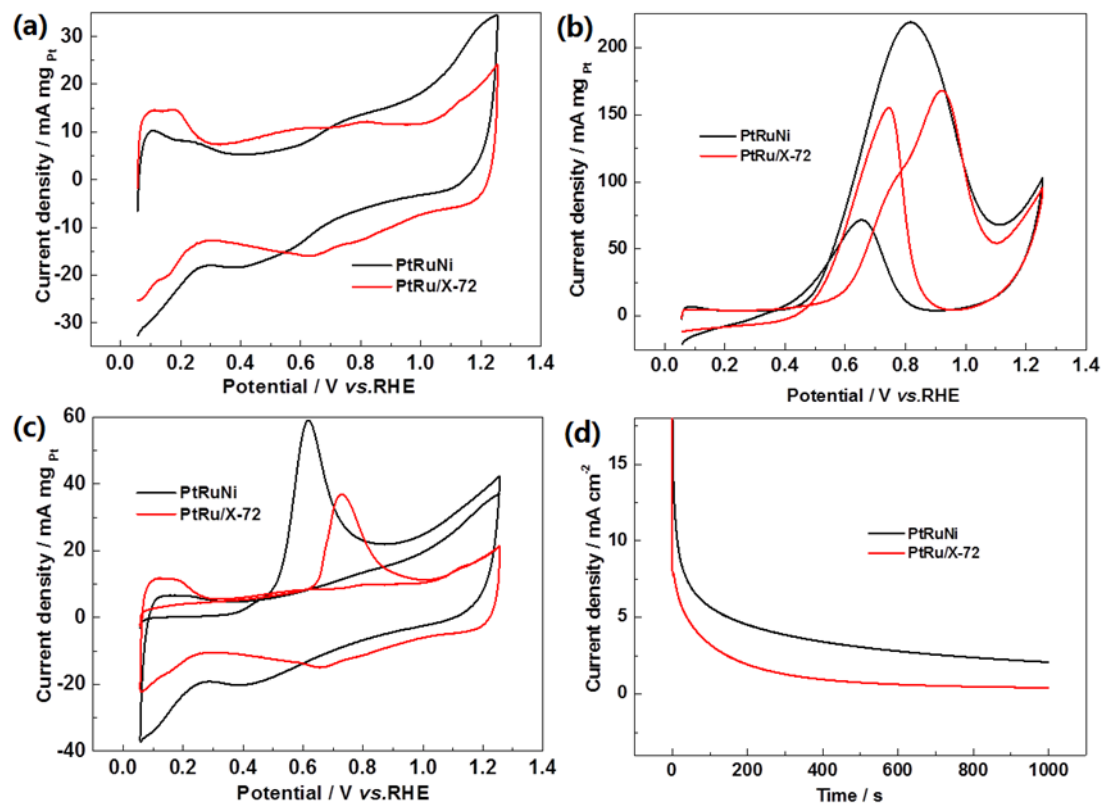


**Figure 2.** Cyclic voltammograms in 0.1 M HClO<sub>4</sub> (a) and 0.5 M CH<sub>3</sub>OH + 0.1 M HClO<sub>4</sub> solution (b) with a scanning rate of 50 mV s<sup>-1</sup>; (c) CO stripping voltammograms in 0.1 M HClO<sub>4</sub> solution with a scanning rate of 50 mV s<sup>-1</sup>; and (d) chronoamperometric curves in 0.5 M CH<sub>3</sub>OH + 0.1 M HClO<sub>4</sub> solution with 0.50 V for PtRuNi networks and PtRu/C catalysts.

**Table 1.** Comparison with the Pt-based catalysts reported in the literature.

Catalysts	Onset potential /(V/RHE)	ECSAs	Reference
PtRuNi networks	0.4	$45.78 \text{ m}^2 \text{ g}_{\text{Pt}}^{-1}$	This work
PtRu/C	0.5	$36.62 \text{ m}^2 \text{ g}_{\text{Pt}}^{-1}$	This work

Pt <sub>7</sub> Ru <sub>2</sub> Fe NWs	0.44	1.10 mA cm <sup>-2</sup>	[15]
PtRu nanodendrites	0.4	40 m <sup>2</sup> g <sub>Pt</sub> <sup>-1</sup>	[16]
PtCu NFs	0.42	18 mA cm <sup>-2</sup>	[17]
Ag@Pt/C-2	0.4	66.1 m <sup>2</sup> g <sub>Pt</sub> <sup>-1</sup>	[18]
PtAu SLAs	0.5	61.90 m <sup>2</sup> g <sub>Pt</sub> <sup>-1</sup>	[19]

The catalytic activity of the catalysts for methanol oxidation was tested in a 0.5 M CH<sub>3</sub>OH+0.1 M HClO<sub>4</sub> solution by CV, in which the current was normalized based on the loading of Pt. As displayed in Figure 2b, the onset potential of methanol oxidation on PtRuNi networks is 0.40 V, a negative shift of 100 mV relative to that of PtRu/C catalysts (0.50 V), confirming that methanol oxidation can readily occur on the PtRuNi network surface. The currents of the oxidation peaks for the PtRuNi networks and PtRu/C catalysts reach 220 mA mg<sub>Pt</sub><sup>-1</sup> and 168 mA mg<sub>Pt</sub><sup>-1</sup>, respectively. The large current response of the PtRuNi network electrode indicates its higher catalytic activity relative to that of PtRu/C catalysts. As shown in Table 1, the PtRuNi catalyst has a lower onset potential than the reported catalysts, PtRuNi networks (0.4 V/RHE), Pt<sub>7</sub>Ru<sub>2</sub>Fe NWs (0.44 V/RHE) PtCu NFs (0.42 V/RHE), PtAu SLAs (0.5 V/RHE).

The CO stripping test was adopted to analyse the toxicity of the catalysts, and the results are shown in Figure 2c. An obvious oxidation peak arises in the first scan, which corresponds to CO oxidation. During the subsequent scan, the CO oxidation peak vanishes due to the complete oxidation of adsorbed CO. The onset potentials of CO oxidation are 0.40 V for PtRuNi networks and 0.65 V for PtRu/C catalysts. A negative shift (approximately 250 mV) of the CO oxidation onset potential demonstrates the higher tolerance of PtRuNi networks than of PtRu/C catalysts. The current response of the CO oxidation reaction reaches the largest value at 0.62 V on the PtRuNi network electrode, while it is 0.73 V on the PtRu/C electrode. This shows that PtRuNi networks are more active for CO oxidation than PtRu/C catalysts. During methanol oxidation, CO is an inevitable intermediate formed during methanol oxidation while simultaneously being a strong poison for the Pt-based electrode, thus reducing activity. The results indicate a more facile CO removal in PtRuNi networks and hence an improved CO tolerance in practice.

The durability of PtRuNi networks was investigated by the chronoamperometry method. The obtained results are plotted in Figure 2d. In the initial period, the current responses of the two electrodes decreased obviously. This implies that the reduction in the number of active sites for catalysis is due to occupation of part of the active sites by the formed CO<sub>ads</sub> and other intermediate products, thus restricting methanol oxidation activity. The currents proceed to decay with time. At approximately 800 s, a pseudo-steady state is achieved. The current on PtRuNi networks is 2.39 mA cm<sup>-2</sup>, approximately 4.9 times that on PtRu/C (0.49 mA cm<sup>-2</sup>), demonstrating a higher Pt utilization of PtRuNi networks.

The presented data suggest that PtRuNi networks have high activity towards methanol oxidation and tolerance for CO. The high activity of PtRuNi networks may result from their unique structure. First, the net framework provides a large surface area and benefits mass transfer, leading to an increase in the catalytic activity of PtRuNi networks. Second, many grain boundaries may act as

active sites for catalysis, and then active sites became more active, causing an increase in the activity of PtRuNi networks.

#### 4. CONCLUSIONS

In summary, PtRuNi networks were investigated by CV. The physical features were characterized by XRD, SEM, and TEM techniques. On the PtRuNi network electrode, the onset potential for methanol oxidation is 0.40 V, which is a negative shift of 100 mV compared to that of commercial PtRu/C, and the mass activity reaches 220 mA mg<sub>Pt</sub><sup>-1</sup> at 0.82 V, an increase of 50 mA mg<sub>Pt</sub><sup>-1</sup> compared to that of commercial PtRu/C. In addition, PtRuNi networks show good durability for methanol oxidation. The good catalytic performance of PtRuNi networks towards methanol oxidation originates from the network structure and the rich grain boundaries.

#### ACKNOWLEDGEMENTS

We thank the National Natural Science Foundation of China (Nos. 21305112 and 21462036) for financial support.

#### References

1. R. Wang, H. Wang, B. Wei, W. Wang, Z. Lei, *Int. J. Hydrogen Energy*, 35 (2010) 10081-10086.
2. R. Wang, Z. Zhang, H. Wang, Z. Lei, *Electrochem. Commun.*, 11 (2009) 1089-1091.
3. W. Wang, Y. Li, H. Wang, Reaction Kinetics, *Mechanisms and Catalysis*, 108 (2013) 433-441.
4. J. Ding, S. Ji, H. Wang, J. Key, D.J.L. Brett, R. Wang, *J. Power Sources*, 374 (2018) 48-54.
5. J. Ding, S. Ji, H. Wang, B.G. Pollet, R. Wang, *Electrochim. Acta*, 255 (2017) 55-62.
6. Y. Ma, H. Wang, W. Lv, S. Ji, B.G. Pollet, S. Li, R. Wang, *RSC Adv.*, 5 (2015) 68655-68661.
7. Y. Ma, R. Wang, H. Wang, J. Key, S. Ji, *RSC Adv.*, 5 (2015) 9837-9842.
8. R. Wang, Y. Ma, H. Wang, K. Julian, S. Ji, *Chem. Commun.*, 50 (2014) 12877-12879.
9. S. Ji, H. Wang, D.J.L. Brett, R. Wang, *Encyclopedia of Interfacial Chemistry*, (2018) 730-738.
10. Y. Ma, H. Li, H. Wang, X. Mao, V. Linkov, S. Ji, O.U. Gcilitshana, R. Wang, *J. Power Sources*, 268 (2014) 498-507.
11. X.T. Zhang, H. Wang, J.L. Key, V. Linkov, S. Ji, X.L. Wang, Z.Q. Lei, R.F. Wang, *J. Electrochem. Soc.*, 159 (2012) B270-B276.
12. Y. Ma, R. Wang, H. Wang, S. Liao, J. Key, V. Linkov, S. Ji, *Materials*, 6 (2013) 1621-1631.
13. L. Gan, M. Heggen, R. Malley, B. Theobald, P. Strasser, *Nano Lett*, 13 (2013) 1131-1138.
14. Y. Ma, H. Wang, S. Ji, V. Linkov, R. Wang, *J. Power Sources*, 247 (2014) 142-150.
15. M. Scofield, C. Koenigsmann, L. Wang, H. Liu, S. Wong, *Energy Environ. Sci.*, 8 (2015) 350-363.
16. S. Lu, K. Eid, D. Ge, J. Guo, L. Wang, H. Wang, H. Gu, *Nanoscale*, 9 (2017) 1033-1039.
17. Z. Zhang, Z. Luo, B. Chen, C. Wei, J. Zhao, J. Chen, X. Zhang, Z. Lai, Z. Fan, C. Tan, M. Zhao, Q. Lu, B. Li, Y. Zong, C. Yan, G. Wang, Z. Xu, H. Zhang, *Adv. Mater.*, 28 (2016) 8712-8717.
18. J. Cao, M. Guo, J. Wu, J. Xu, W. Wang, Z. Chen, *J Power Sources*, 277 (2015) 155-160.
19. J. Feng, L. He, R. Fang, Q. Wang, J. Yuan, A. Wang, *J Power Sources*, 330 (2016) 140-148.